

# Fabrication of Three-Dimensional Micro-Structures in Glass by Picosecond Laser Micro-Machining and Welding

Krystian L. WLODARCZYK, Richard M. CARTER, Amir JAHANBAKHS, Duncan P. HAND, Robert R. M. MAIER, and Mercedes MAROTO-VALER

*School of Engineering and Physical Sciences, Heriot-Watt University,  
Edinburgh, EH14 4AS, United Kingdom  
E-mail: K.L.Wlodarczyk@hw.ac.uk*

This paper describes a relatively inexpensive laser-based process for the fabrication of enclosed three-dimensional micro-structures in borosilicate glass substrates. The micro-structures will be used as customized ‘models’ of subsurface systems for the investigation and the validation of simulations of gas/liquid flow and reactive transport processes occurring in porous media at the pore scale level. The fabrication process of these microfluidic devices uses the same picosecond laser for the generation of micro-structures on glass and for sealing the structures with another glass plate. The laser processing parameters used for micro-machining and welding of glass substrates are described, and the challenges associated with the overall manufacturing process discussed.

**Keywords:** Ultrashort pulsed laser, micro-machining, micro-welding, glass, microfluidic devices.

## 1. Introduction

The high transparency, thermal stability, hardness, chemical resistance and chemical inertness of glass often make this material a preferred substrate over silicon or polymers for the manufacturing of microfluidic devices, in particular for applications in advanced chemistry, biology, medicine and geological research [1].

The conventional manufacturing of glass-based microfluidic devices is a complex, multi-step process that utilizes photolithography, wet etching and anodic bonding [2]. The combination of photolithography and etching processes enables the precision generation of micro-structures, such as micro-channels and reservoirs, on the surface of glass. Although this fabrication method enables the generation of optically-smooth surfaces (with Ra values < 10nm) and steep (almost vertical) walls [3], the etching process permits the manufacturing of only two-dimensional structures (i.e. all etched features have a constant depth). Moreover, low etching rates (less than 1µm per minute) and the requirement of using customized masks make this process rather slow and expensive, and hence less desirable for rapid prototyping of microfluidic devices at low volume. Another drawback of the etching process is the use of hazardous chemicals (e.g. hydrofluoric acid HF) that are often toxic and dangerous to work with.

Anodic, also known as electrostatic or field-assisted bonding, is commonly used to seal the etched glass structures to either silicon or a metal plate without using any intermediate bonding layer. Anodic bonding of two glass substrates is also feasible, but then a thin (typically < 1µm) metallic or silicon-based layer must be applied between the glass substrates prior to bonding [4]. This, unfortunately, limits the optical access to the etched micro-channels from the metallic side. Furthermore, successful anodic bonding can only be achieved if the surfaces are very clean and flat in order to ensure atomic contact between the bonding substrates through a sufficiently powerful electrostatic field.

This paper presents a novel laser-based approach for the fabrication of enclosed glass-based microfluidic devices using a single tool, making the fabrication process very attractive for rapid prototyping of microfluidics at low cost. The entire fabrication process is performed with a single ultrashort-pulsed laser which is used both for the generation of micro-structures on glass and for sealing the structures with another glass plate, without using any intermediate bonding layers. Ultrashort-pulsed lasers have been demonstrated as effective tools for micro-machining a wide range of materials, including glass which is normally transparent for most lasers [3, 5-9], as well as for joining glass to glass [10-14] or even glass to metal [14, 15].

In this paper, for the first time, we demonstrate a purely laser-based fabrication process of enclosed 3D micro-structures in glass. We believe that this process in the future can be used as an alternative fabrication approach for rapid prototyping of microfluidics. In our case, we aim to use such enclosed micro-structures as ‘physical models’ of subsurface systems to investigate fluid flow and reactive transport at the pore scale level.

## 2. Experimental

### 2.1 Glass substrate

The microfluidic devices presented in this paper have been fabricated from 1.1mm thick Schott Borofloat®33 glass substrates. This glass contains 81% of SiO<sub>2</sub>, 13% of B<sub>2</sub>O<sub>3</sub>, 4% of Na<sub>2</sub>O/K<sub>2</sub>O, and approximately 2% of Al<sub>2</sub>O<sub>3</sub> [16]. This floated borosilicate glass has similar optical properties to fused silica, but it is less expensive. It is used in many industrial and scientific areas, e.g. chemistry, optics, micro-electronics, photovoltaics and biotechnology.

### 2.2 Laser micro-machining system

Figure 1 shows the laser setup used for the generation of micro-structures on the glass surface. The laser source is

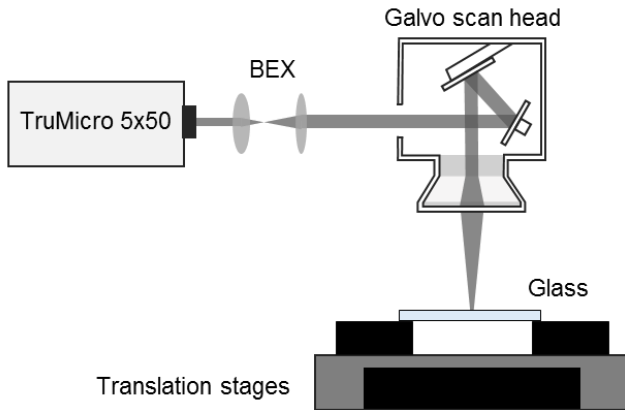


Fig. 1. Laser setup used for micro-machining glass substrates.

a 50W Trumpf TruMicro 5x50 laser that provides 6ps long pulses (FWHM). The laser has three outputs, enabling processing of different materials at one of the three available wavelengths ( $\lambda$ ): 1030nm, 515nm, or 343nm. Laser pulses can be provided with a maximum pulse repetition frequency (PRF) of 400kHz. The laser beam is delivered to the work piece via a galvo scan head and a 160mm focal length F-theta lens. The laser beam delivery is very similar for each wavelength. The focused laser beam diameters were measured (at  $1/e^2$  of its maximum intensity) to be  $20\mu\text{m}$  at  $\lambda = 343\text{nm}$ ,  $20\mu\text{m}$  at  $\lambda = 515\text{nm}$ , and  $35\mu\text{m}$  at  $\lambda = 1030\text{nm}$ .

The borosilicate glass substrates have been machined at the 515nm wavelength; chosen because at this wavelength the material is machined efficiently at a relatively high resolution and processing speed. Laser processing was carried out in air. The mounting arrangement for the glass provided a clear aperture underneath the machining region.

### 2.3 Laser micro-welding setup

The same laser has been used for sealing the laser-generated micro-structures with another glass plate without using any intermediate joining layers. This time, however, the laser process was carried out at the 1030nm wavelength, using a stationary laser beam delivered via a 10mm focal length lens (NA 0.5).

In order to successfully bond two glass plates together, the picosecond laser pulses with a PRF of 400kHz were propagated through the first (blank) glass, and focused to a very small (approx.  $3\mu\text{m}$  diameter) spot slightly below (approx.  $100\mu\text{m}$  underneath) the glass-glass interface. Due to the nonlinear interactions at the focus, the laser beam generated a localized heated zone (in both glass plates) and a plasma that mixed the molten glass to form a solid 'tear-shaped' join.

The key challenge in laser micro-welding is to bring the two glass plates into sufficiently close contact that they are both within the effective focal depth of the laser and can confine the plasma once it is generated [14]. Too large a gap between the two materials allows the plasma to escape and ablation rather than a weld formation occurs.

Ideal optical contact without a gap between the two glass plates can be achieved when both glass surfaces are perfectly clean and flat. Then it is only necessary to place one glass on top of the other and Van der Waals forces are

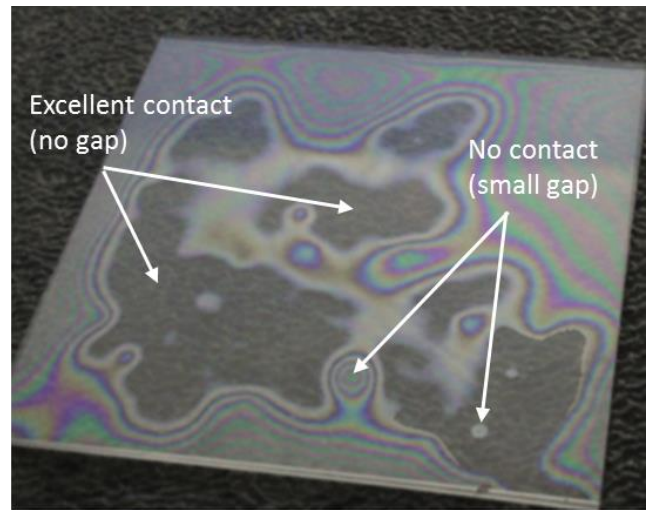


Fig. 2. Inappropriate preparation of glass samples for welding.

capable of holding the two materials together. Unfortunately, in reality such a scenario is unlikely to happen because the glass substrates are often contaminated by dust and possess surface imperfections, such as little surface waviness or chips at glass edges, which often lead to the creation of gaps at the glass-glass interface. Then it is necessary to carefully clean the glass substrates before placing them on top of the other and to use a force to obtain optical contact (i.e. a gap of  $< 0.25$  of the wavelength) between them. Figure 2 shows a sample with partially good contact between the two glass plates, indicating the areas of optical contact and the areas containing small gaps (e.g. due to dust particles).

The laser setup used for sealing the laser generated micro-structures with the other (blank) glass plate is shown in Fig. 3. Prior to laser micro-welding, the glass surfaces were carefully cleaned using lens tissues saturated with methanol and then dried by a stream of ionized nitrogen. This provides effective removal of the dust particles before forcing the glass plates into optical contact. To maintain this con-

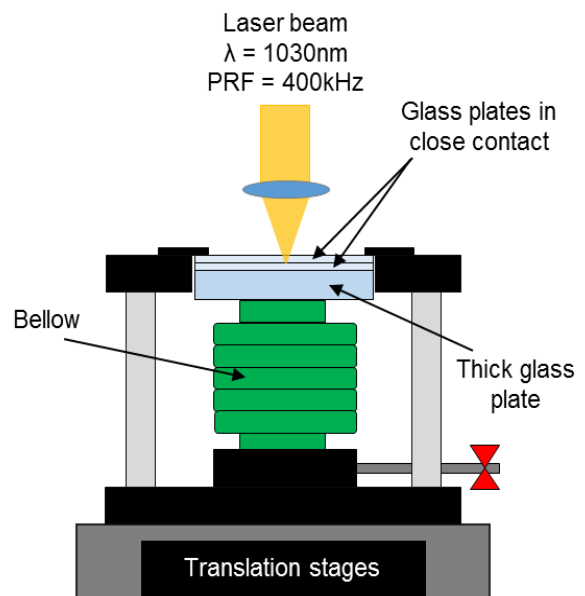


Fig. 3. Laser setup used for joining two glass plates together.

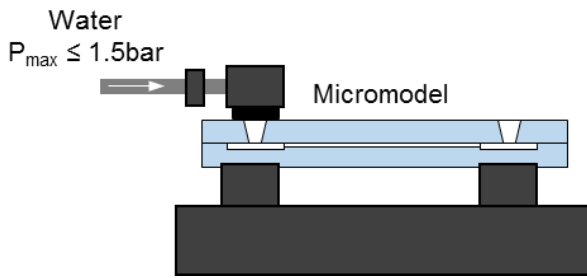


Fig. 4. Hermeticity test of the micromodel.

tact during the laser micro-welding process, the two materials were later clamped together by use of a pneumatic piston (bellow) that was pressurized to approximately 1bar. To ensure a uniform pressure across the glass plates and avoid damage of the bellow by a focused laser beam, a 9mm thick glass plate was inserted between the second glass plate and the bellow.

### 2.4 Testing rig

The hermeticity of the laser-generated enclosed micro-structures was tested using the simple setup shown in Fig. 4. The test was performed by injecting a tap water into the micro-structure channels through one of the two inlets that were generated in the cover (top) glass using the picosecond laser. The water was injected at pressures of up to 1.5bar.

## 3. Results

### 3.1 Laser micromachining results

Figure 5 shows an example of a micro-channel produced on the surface of Borofloat®33 glass by using picosecond laser pulses of energy ( $E_p$ ) 34.4 $\mu$ J. This micro-channel was measured to be 14 $\mu$ m deep and 14 $\mu$ m wide (at FWHM). In comparison to the chemically-etched micro-channels, this example does not have steep walls (due to the Gaussian shape of the laser beam intensity profile) and smooth surfaces (with a typical Ra value of 0.9 $\mu$ m as measured for 0.2mm long channels).

The depth of the micro-channels can be controlled by the laser pulse energy, scanning speed, and the number of

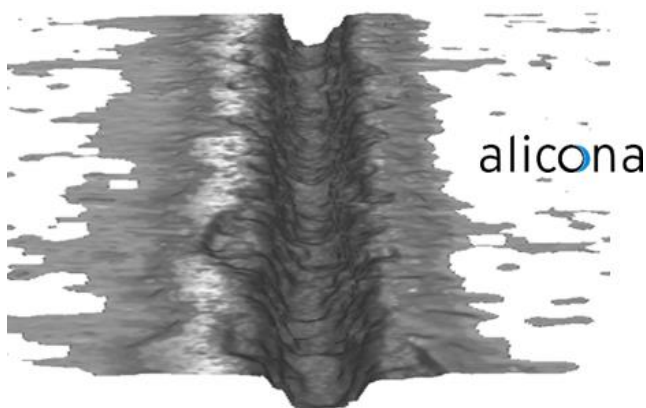


Fig. 5. Example of the laser-generated micro-channel: 14 $\mu$ m deep and 14 $\mu$ m wide (measured as FWHM). This channel was measured using an Alicona 3D surface profilometer.

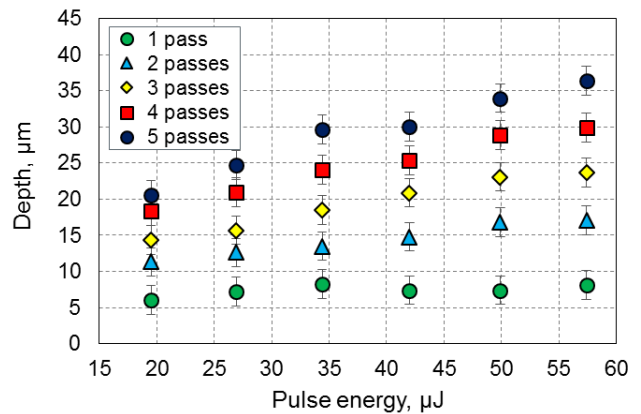


Fig. 6. Depth of micro-channels generated at different value of laser pulse energy. Results presented for a different number of laser beam passes.

laser beam passes. Figure 6 shows that the depth of the micro-channels increases in almost a linear manner with increasing pulse energy, and the micro-channels with a depth of up to 40 $\mu$ m can be produced by applying multiple laser beam passes. The width of these micro-channels can be as small as 14 $\pm$ 3 $\mu$ m, as measured at FWHM by using a 3D surface profilometer (InfiniteFocus® Alicona).

Small reservoirs can also be generated on the surface of Borofloat®33 glass by using a picosecond laser. Figure 7 shows a 1mm  $\times$  1mm  $\times$  50 $\mu$ m deep pocket that was generated by raster scanning the laser beam at a 150mm/s speed and 26.9 $\mu$ J pulse energy. The spacing distance between the scanning lines was chosen to be 3.6 $\mu$ m. The surface roughness ( $S_a$ ) within a 0.8mm  $\times$  0.8mm machined area was measured to be approximately 1.8 $\mu$ m (using the Alicona surface profilometer).

The depth of the reservoirs can be controlled by applying laser pulses of an appropriate energy, as can be seen in Fig. 8. The spacing distance between the scanning lines also was found to have a significant impact on the ablation depth. The results in Fig. 8 demonstrate that the ablation depth can be well controlled by adjusting the pulse energy and the spacing between the laser beam scan lines.

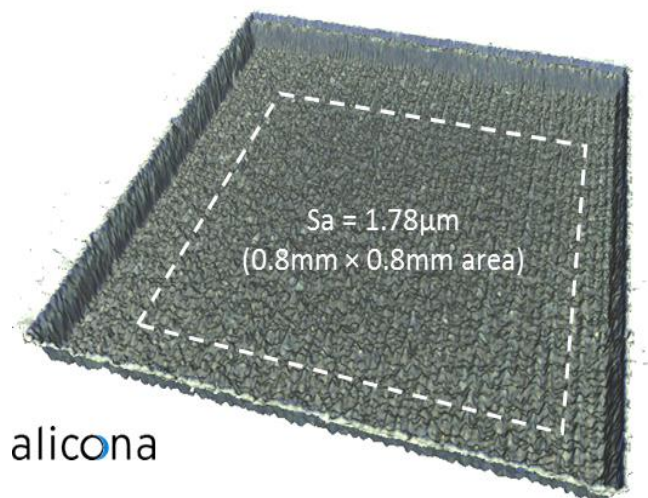
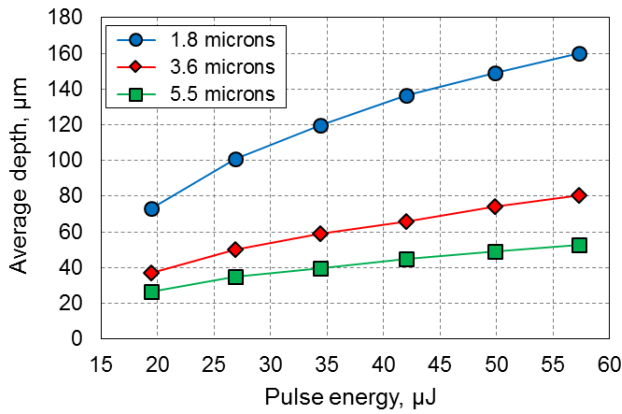


Fig. 7. Example of the picosecond laser-machined area, generated at pulse energy of 26.9 $\mu$ J.





**Fig. 8.** Average depth of the laser machined areas obtained with different values of pulse energy. Results are presented for three different values of spacing between the laser beam scan lines.

### 3.2 Laser welding results

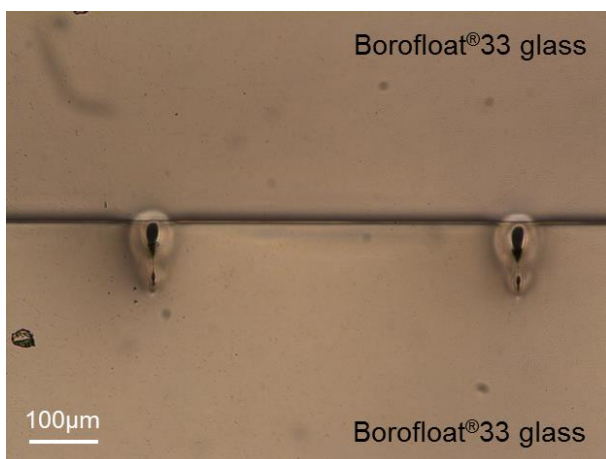
Successful welds were generated by focusing the laser radiation a 100µm distance below the glass-glass interface, moving the samples with a 2mm/s scan speed. An average laser power used for welding was 2W.

Figure 9 shows a cross-section of the laser-generated welds that were measured to be approximately 140µm long and 80µm wide. The cross-section view was obtained by dicing the laser-welded glass plates, polishing the facets, and imaging by using a Leica optical microscope.

### 4. Fabrication and testing of microfluidics

A microfluidic device manufactured using the picosecond laser processes described above is shown in Fig. 10. This device contains a grid of 16µm deep and 14µm wide micro-channels and two 5mm × 5mm reservoirs that are connected with the grid via two 1mm wide and 10mm long channels. The reservoirs along with channels are normally used for delivering fluids and/or gases to the area of interest, i.e., the grid of micro-channels.

Here, it must be noticed that the microfluidic device shown in Fig. 10 does not have an external access to the pockets through which fluids and/or gasses can be injected. In our later microfluidic devices, such access was provided by drilling small holes in the cover (top) glass plate using the picosecond laser.



**Fig. 9.** Cross-section of the welds.

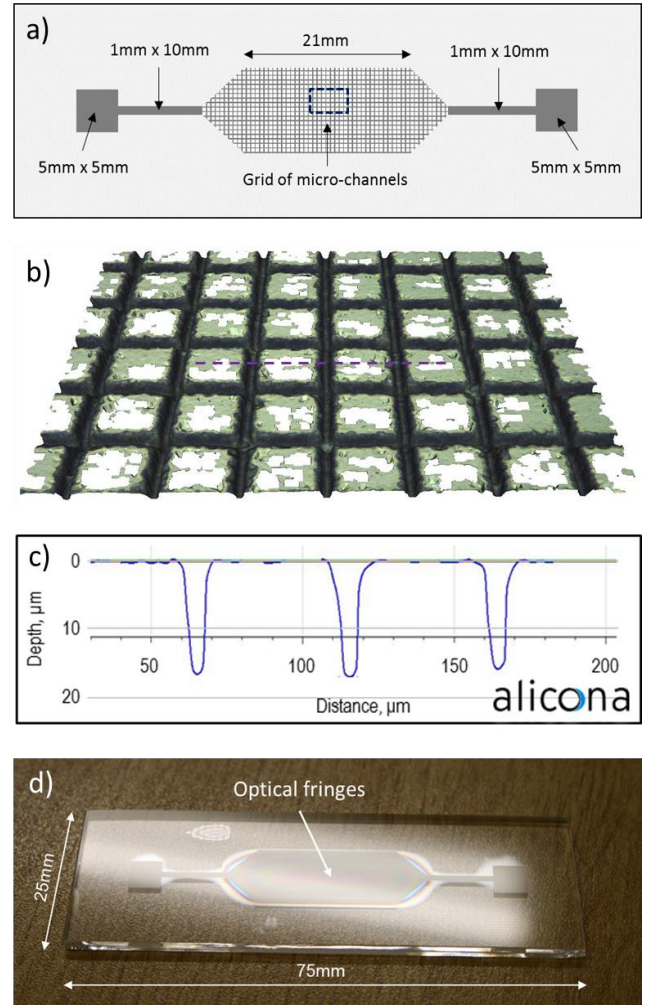


**Fig. 10.** Microfluidic device fabricated by using a picosecond laser: a) design, b) Alicona 3D surface profile of the grid of micro-channels, c) cross-section of the micro-channels, d) photograph of the manufactured microfluidic device.

One of the challenges in the laser-based manufacturing of microfluidic devices is avoidance of debris and surface contamination produced during the laser micro-machining process. Such debris and contaminants can be very difficult to remove following machining, in particular these debris that firmly stick to the glass surface.

Figure 10d) shows a case when a glass substrate affected by the laser-induced debris was welded to the other glass plate. Although the welds were successfully generated everywhere around the laser-machined area, thereby closing nearly all air gaps between the two glass plates, inside and near the laser-machined area the air-gaps were left unclosed. The gaps are indicated by optical fringes, also known as Newton's rings.

The fluid flow tests performed on the laser-generated microfluidic devices has shown that the welds provided a good sealing of the micro-structures, i.e. water leakage was not detected, even though water was injected to the micro-channels at 1bar pressure. During the test, it was noticed that the positive pressure applied to the micro-structure was able to increase slightly the gap within the laser-machined area. This was observed because the optical fringes started to move. Since we did not use dyed water, we were not

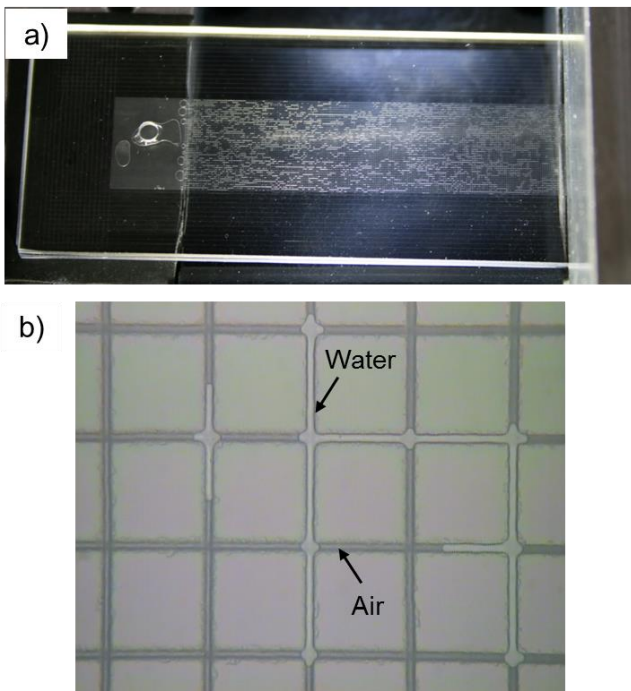


**Fig. 11.** Microfluidic devices during the fluid flow test experiment: a) photograph and b) optical microscope image showing some micro-channels filled in with water.

able to confirm if the gaps were sufficiently large for the fluid to flow into them.

Figure 11a) shows the distribution of water within the grid of micro-channels while performing one of the fluid flow test experiments. Under the optical microscope objective, as shown in Figure 11b), it was possible to clearly differentiate between those micro-channels filled in with water and those still filled in with air.

## 5. Conclusions

This paper has demonstrated a relatively inexpensive laser-based process for the manufacture of enclosed glass-based microfluidics. The liquid fluid tests have proven that a good sealing of the micro-structures can be achieved by a picosecond laser welding process. The optical fringes that were clearly visible indicate that there is a small (approximately a couple of  $\mu\text{m}$ ) gap between the laser-machined area and the cover glass substrate. This gap results from the laser-generated debris. In order to remove these debris, the glass substrates have to properly clean following the laser micro-machining process either using chemical or thermal treatment. The fabricated micro-structures are planned to

be used as customized ‘models’ of subsurface systems for the investigation of various processes occurring inside porous media (e.g. rocks) at the pore scale level.

## Acknowledgments

This project has received funding from the European Research Council (ERC) under the European Union’s Horizon 2020 research and innovation programme (MILEPOST, Grant agreement no.: 695070). This paper reflects only the authors’ view and ERC is not responsible for any use that may be made of the information it contains.

## References

- [1] C.G. Khan Malek, *Anal. Bioanal. Chem.* 385 (2006), 1351-1369.
- [2] C. Iliescu, H. Taylor, M. Avram, J. Miao, S. Franssila, *Biomicrofluidics* 6 (2012), 016505-1-16
- [3] S. Queste, R. Salut, S. Clatot, J.-Y. Rauch, C.G. Khan Malek, *Microsyst. Technol.* 16 (2010), 1485-1493.
- [4] A. Berthold, L. Nicola, P.M. Sarro, M.J. Vellekoop, *Sens. Actuators A.* 82 (2000), 224-228.
- [5] K.L. Wlodarczyk, W.M. MacPherson, D.P. Hand, “Laser processing of Borofloat®33 glass,” *Proc. 16th Int. Symp. on Laser Precision Microfabrication (LPM)*, Kokura, Japan (May 2015).
- [6] K.L. Wlodarczyk, A. Brunton, P. Rumsby, D.P. Hand, *Opt. Lasers Eng.* 78 (2016), 64-74.
- [7] S. Nikumb, Q. Chen, C. Li, H. Reshef, H.Y. Zheng, H. Qiu, D. Low, *Thin Solid Films* 477 (2005), 216-221.
- [8] K. Sugioka, Y. Cheng, *Light Sci. Appl.* 3 (2014), 1-12.
- [9] C. Moorhouse, *Phys. Procedia* 41 (2013), 381-388.
- [10] J. Chen, R.M. Carter, R.R. Thomson, D.P. Hand, *Opt. Express* 23 (2015), 18645-18657.
- [11] I. Miyamoto, K. Cvecek, Y. Okamoto, M. Schmidt, *Appl. Phys. A.* 114 (2014), 187-208.
- [12] K. Cvecek, R. Odatto, S. Dehmel, I. Miyamoto, M. Schmidt, *Opt. Express* 23 (2015), 5681-5693.
- [13] W. Watanabe, Y. Li, K. Itoh, *Opt. Laser Technol.* 78 (2016), 52-61.
- [14] R.M. Carter, J. Chen, J.D. Shephard, R.R. Thomson, D.P. Hand, *Appl. Opt.* 19 (2014), 4233-4238.
- [15] R.M. Carter, M. Troughton, J. Chen, I. Elder, R.R. Thomson, M.J.D. Esser, R.A. Lamb, D.P. Hand, *Appl. Opt.* 56 (2017), 4873-4881.
- [16] “Borofloat®33 – Borosilicate glass,” <http://www.schott.com/borofloat/english/>.